# Charge-switchable Metal-organic Framework for Size/Charge-selective Molecular Inclusions

YUAN Bei-Bei[1,2,3], ZHOU Bei-Bei[1,2,3], ZHANG Yue-Biao[1,3], SHI Jian-Lin[1,2,3]

(1. School of Physical Science and Technology, ShanghaiTech University, Shanghai 201210, China; 2. Shanghai Institute of Ceramics, Chinese Academy of Sciences, Shanghai 200050, China; 3. University of Chinese Academy of Sciences, Beijing 100049, China)

**Abstract:** Highly size/charge-selective molecular inclusions by a charge-switchable zinc-based metal-organic framework (Zn-MOF) have been achieved, which comprises of two kinds of paddle-wheel building units and four kinds of nanocages. Featuring counter anions floating in the pore and accessible coordination sites on the skeleton, Zn-MOF represents exceptional versatility in taking up anionic dyes by ion-exchange, cationic dyes by charge switch of skeleton, and neutral organic dyes by host-guest interactions. Both size and charge selectivities in the molecular inclusion by the charged nanocages in Zn-MOF provide an efficient way in designing superior porous materials with an enhanced level of compatibility and recognition.

**Key words:** metal-organic framework; charge-switchability; molecular inclusion; selectivity

Metal-organic frameworks (MOFs) are designable crystalline porous materials by stitching inorganic building blocks with tailored organic linkers, which offer a higher level of heterogeneity in compositions and richness of host-guest interactions for molecular inclusions. The versatility to encapsulate a large variety of molecules are highly desired properties for porous materials in molecular sensing[1-2], molecular separation[3-4], heterogeneous catalysis[5], biomedical diagnosis and drug delivery[6-7], and removal of organic pollutants[8-9].

Several mechanisms have been proposed for molecular inclusion driven by ion-exchange[10], $\pi-\pi$ interaction, hydrogen bonding, electrostatic interaction[11], and open metal sites within MOFs[12]. Up to date, the rational design of MOFs with exceptional versatility for molecular inclusion remains largely unestablished[13]. Thus, it rises the need of mechanism studies for dye adsorption in diverse MOF systems.

Generally, the neutral zinc-based MOF-5 crystal can encapsulate both neutral and cationic dyes but not anionic dyes[14]. ZIF-8 tends to absorb a small amount of dyes on the surface because of the charged sites at the external surface[15-16]. Anionic zinc-based MOFs tend to encapsulate cationic dyes[17-18]. Herein, we have studied the dye adsorption properties and related mechanisms of a MOF comprising of charged nanocages, with versatility in taking up neutral, cationic, and anionic molecules with size selectivity controlled by the cages. Featuring nitrate ($NO_3^-$) as the counter ions floating within the pore of the MOF, the inclusion of anionic dyes was accelerated with the ion-exchange mechanism. The release experiments of dye@Zn-MOF show a faster rate of salt flowing out in the NaCl solution compared to that in $Et_4N^+BF_4^-$ solution, indicating the anionic dyes are more easily exchanged with the smaller sized anion. Size selectivity and adsorption kinetics for anionic dye inclusion have also been performed. More interestingly, the inclusion of cation dyes by the cationic framework is actually going through a charge-switch process by the Cl⁻ from the dyes coordinated to the metal centers in the frameworks. As evidence, the cationic dye release experiments show a slower rate of migration when salting out in a NaCl solution compared to that in $NaNO_3$ solution. The adsorption of neutral dyes relies on the porosity of the framework and supramolecular interactions. The competing adsorptions of cationic and neutral dyes have shown that the electrostatic interaction is the dominating process. The heterogeneity and multi-pathway endow MOFs with the versatility to take up a large variety of molecules, which can inspire more intelligent design of MOFs with higher level of compatibility and recognition.

# 1  Experimental

## 1.1  Materials and instruments

All of the chemicals were obtained from commercial source. The single-crystal X-ray diffraction data (CCDC-1814467-1814468) were obtained at beamline BL17B of the Shanghai Synchrotron Radiation Facility (SSRF) using X-ray with a wavelength of 0.12398 nm. The PXRD patterns were collected on a Bruker Advance D8 diffractometer using Cu-K$\alpha$ radiation ($\lambda$ = 0.154050 nm) at 40 kV and 40 mA, at a scanning rate of 2.3°/min and $2\theta$ range of 3°−30°. The UV-Vis spectra were collected on an Agilent Carry 5000 spectrophotometer.

## 1.2  Preparation of compounds

$[Zn_{14}(L)_4(H_2O)_{22}](NO_3)_4(DMF)_x$: In a 20 mL scintillation vial, 209 mg $H_6L$ (0.3 mmol) and 627.5 mg $Zn(NO_3)_2\cdot4H_2O$ (2.4 mmol) were dissolved in 16 mL DMF solution. The vial was sealed and placed in 85℃ for 48 h. Colorless pyramidal crystals were obtained after cooling down to room temperature.

$[Co_{14}(L)_4Cl_3(H_2O)_{22}]Cl(DMF)_x$: In a 20 mL scintillation vial, 209 mg $H_6L$ (0.3 mmol) and 571 mg $CoCl_2\cdot6H_2O$ (2.4 mmol) were dissolved in 16 mL DMF solution. The vial was sealed and placed at 85℃ for 48 h. Blue-black pyramidal crystals were obtained after cooling down to room temperature.

## 1.3  Absorption experiment of organic dyes

The freshly prepared Zn-MOF single crystals were washed with DMF for three days and three times per day, then washed with MeOH for five days and three times per day to remove the DMF. For each dye-absorption experiment, 50 mg Zn-MOF samples were soaked in a 10 mL dye/MeOH solution in a 20 mL vial. After an interval of a certain time, the upper solution was taken for UV-Vis spectra monitor. The absorbance value of the dye/MeOH solution at 0 h was normalized as 100% in the UV-Vis spectra.

## 1.4  Release experiment of organic dyes

After Zn-MOF samples were soaked in the 10 mL dye/MeOH solution for 48 h, the upper solution was removed and absorption process was terminated. Then the dye@Zn-MOF samples were washed with 5 mL anhydrous methanol for several times until there is no leaching of dyes. Then the dye@Zn-MOF samples were transferred into 10 mL salt/MeOH solution. The system was stirred on a shaker for well mixing. After an interval of a certain time, the upper solution was taken for UV-Vis spectra monitor, and then poured back to keep the original system unchanged.

# 2  Results and discussion.

## 2.1  Crystal Structure

The crystal structure of the Zn-MOF was first reported by Hong, *et al*[19], whose property is highly deserved further exploitation. Sought to use this MOF as a model compound, we have optimized the synthetic condition, obtained sufficiently large size crystals and investigated the precise crystal structure by synchrotron radiation diffraction (Fig. S1).

The Zn-MOF composes four kinds of polyhedral cages including rhombicuboctahedral, cuboctahedral, truncated octahedral, and square-bifrustum cages (Fig. S2). All the cages are bearing positive charges, except the truncated tetrahedral one. The $NO_3^-$ counter anions were found floating in the pores determined by the single-crystal diffraction analysis in this work. This result is different from the crystal structure of the Zn-MOF made from DMSO with the $OH^-$ as counter anion. Regardless of the counter anions and guest molecules, the nanocages possess large voids having the diameters of 1.31 nm (Fig. S2(a), yellow), 0.96 nm (Fig. S2(b), pink), 1.64 nm (Fig. S2(c), green), and 0.92 nm × 0.92 nm × 1.4 nm (Fig. S2(d), orange), respectively.

## 2.2  Organic dye adsorption by Zn-MOF single crystals

To visualize the versatility for molecular inclusion, 13 organic dyes with various sizes and charges (Table S1) were used in the adsorption experiments in MeOH solutions, including two neutral (SY2 and SD1), four cationic ($MLB^+$, $BF^+$, $CV^+$, and $R6G^+$), and seven anionic dyes ($MO^-$, $TOO^-$, $AO7^-$, $AR88^-$, $AB1^-$, $OG^{2-}$, and $NC^{3-}$). The dye adsorption behaviors were examined by optical microscopy of the single crystals of the Zn-MOF with sufficiently large sizes (Fig. S3).

Surprisingly, the Zn-MOF crystal is able to take up neutral, cationic and anionic dyes without changing the original crystal structure (Fig. S4), judging from the exterior and interior of the crystals after immersing in the dye solutions for several hours. It is a rare case for a zinc-based MOF crystal. To the best of our knowledges, there are only a few MOFs can take up both cationic and anionic dyes. The typical example is the inclusion of $MLB^+$ and $MO^-$ in MOF-235[13]. By controlling the pH of solution and creating different zeta potential on the surface of MOFs, MOFs like PCN-222[20], MIL-100(Fe) and MIL-100(Cr)[21] can absorb cationic and anionic dyes (Table S2).

## 2.3  Anionic dye inclusion pathway

Since the Zn-MOF contains counter anions in the nanocages, it is hypothesized that the anionic dye inclu-

sion is an ion-exchange process. Due to the difficulty to analyze the content of nitrate anion in the solution, we use the multicycle adsorption method to study the dye inclusion behavior. As shown in Fig. 1(a), $AO7^-$ was used as a probe to monitor the adsorption kinetic of Zn-MOF, which showed rapid uptake at the beginning and reached equilibrium after 30 h. The $AO7^-$ solution was refreshed to break this equilibrium, and found a second step of dye uptake. Such behavior reveals the concentration gradient is a driving force for dye inclusion, besides the host-guest interaction such as π-π interaction and electrostatic interaction.

To further testify the ion-exchange process in anionic dyes inclusion, the NaCl and $Et_4N^+BF_4^-$ solution were used for salting out experiment, respectively. As shown in Fig. 1(b), when immersing the crystal of $AR88^-@$Zn-MOF into the same concentration methanol solution of NaCl and $Et_4N^+BF_4^-$ (0.18 mol/L), the $AR88^-$ will be released out from the crystals monitoring from the increasing absorbance intensity of $AR88^-$ at 509 nm. Compared with the release of $AR88^-$ in $Et_4N^+BF_4^-$, the dye release process in the NaCl solution is slower, which is due to the larger size and slower diffusion of $BF_4^-$.

The size selectivity of Zn-MOF is illustrated by the anionic dyes adsorption. Larger size or more charges dyes such as $AB1^-$ (1.67 nm × 1.333 nm × 1.12 nm), $OG^{2-}$ (1.11 nm × 1.263 nm × 0.496 nm), and $NC^{3-}$ (1.27 nm × 1.22 nm ×1.04 nm³) penetrated only on the outer part of the crystals. It is clear that the $AB1^-$ has a dimension exceed the size of nanocages in the framework, revealing the capability for exclusive size separation of molecule. To demonstrate the exclusive dye separation, selective anion exchange with the framework was investigated by performing anion-exchange experiments with a green color binary mixture solution of $TOO^-$ and $AB1^-$ (molar ratio 1∶765). As shown in Fig. 2(a), the mixture solution turns into blue after selective inclusion $TOO^-$ over $AB1^-$ by Zn-MOF. Figure 2(b) shows the rapid drop of $TOO^-$ and the retention of $AB1^-$ in the solution.

## 2.4 Cationic dyes inclusion pathway

The exterior and interior optical microscope images of $MLB^+@$Zn-MOF and the time dependent UV-Vis spectra of $MLB^+$ solution with Zn-MOF single-crystals (Fig. S5) indicated $MLB^+$ were included within the MOF. Here the $Cl^-$ from dyes coordinated to the metal centers in the frameworks, thus turns the charge of the framework into
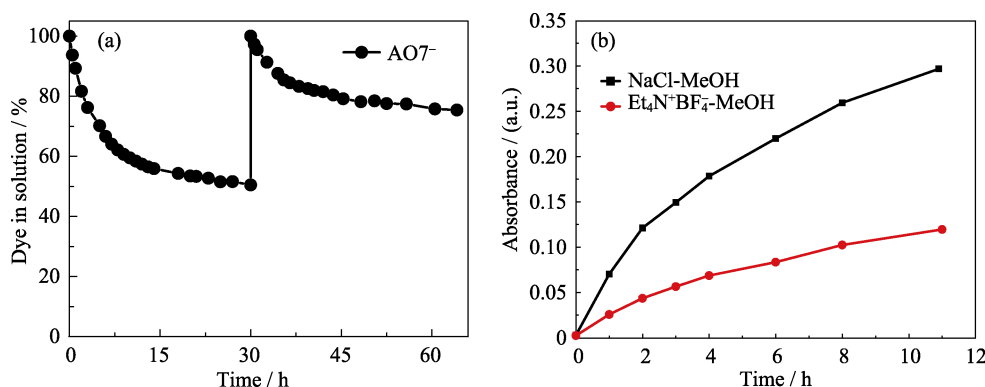


Fig. 1 (a) Dye adsorption kinetics of $AO7^-$ by Zn-MOF, which was immersed into a fresh $AO7^-$ solution at 30 h for second uptake, indicating that the concentration gradient potential served as the driving force for dye inclusion; (b) Release rates of $AR88^-$ (at $\lambda_{max}$ = 509 nm) salt out from $AR88^-@$Zn-MOF in 0.18 mol/L methanol solution of NaCl and $Et_4N^+BF_4^-$, respectively
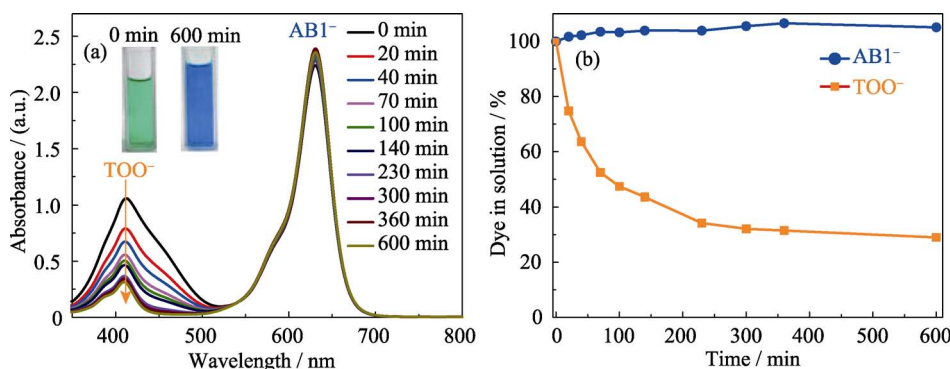


Fig. 2 (a) The time dependent UV-Vis spectra of the solutions of $AB1^-$ and $TOO^-$ in the ratio of 765∶1 for the competitive adsorption by Zn-MOF ($\lambda_{max}$= 412 nm for $TOO^-$, $\lambda_{max}$= 630 nm for $AB1^-$) with inset showing the colour of $TOO^-/AB1^-$ solution before and after dye inclusion for 600 min, respectively; (b) The adsorption kinetics of $AB1^-$ and $TOO^-$ by Zn-MOF in the binary mixture solution
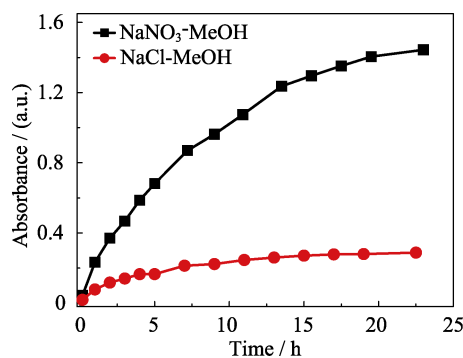
**Fig. 3** Release profiles of MLB$^+$ (at $\lambda_{max}$ = 648 nm) salt out from MLB$^+$@Zn-MOF in saturated methanol solution of NaNO$_3$ and NaCl, respectively

anionic for the incorporation of cationic dyes. This can be supported by the fact that the counter ions Cl$^-$ are bonding to the metal centers in [Co$_{14}$(L)$_4$Cl$_3$(H$_2$O)$_{22}$] Cl(DMF)$_x$. Salting out method was tried to investigate the different control of dyes release in the Zn-MOF. As shown in Fig. 3, when immersing the crystal of MLB$^+$@ Zn-MOF into the saturated MeOH solution of NaCl, the MLB$^+$ will be released out from the crystals monitoring from the increasing absorbance of MLB$^+$ at 652 nm. Obviously, the dye release rate in saturated methanol solution of NaCl solution is slower than that in NaNO$_3$ solution. This result supports the charge-switch mechanism for dye absorption.

## 2.5 Adsorption kinetics difference between charged and neutral dyes.

To study the influence of electrostatic interaction to the dye adsorption kinetics, MLB$^+$ and SY2 were chose for the competitive inclusion experiments considering the similar molecule sizes but different UV-Vis adsorption wavelengths. As shown in Fig. 4(a), the UV-Vis spectroscopy of the mixed dyes solution exhibits that the absorbance gradually decreased at 652 nm, but remained at 406 nm over 31 h. The dye retention plot (Fig. 4(b)) shows the drop of MLB$^+$ concentration in contrast with

the almost constant concentration of SY2. Zooming in the plot, it can be seen that an initial simultaneous uptake of both MLB$^+$ and SY2, in which the adsorbed SY2 was further kicked out by the MLB$^+$. Such observation indicates that Zn-MOF has faster adsorption rate for charged MLB$^+$ compared with that of the neutral SY2. It was also observed that neutral dyes could be released in neat MeOH, while charged dyes would not be released after adsorbed in the Zn-MOF. The difference of the host-guest interaction can be well understood by the electrostatic interaction, which induces faster kinetics and selective adsorption of charged dyes. This phenomenon is very useful for selective adsorption and kinetic separation for large molecules.

## 3 Conclusions

In this work, the molecular uptake and release behaviours of a model MOF comprising charged polyhedral nanocages toward a series of dyes with varied sized diameters and different charges have been explored. With the cage-type and charged structural features, the Zn-MOF represents excellent size selectivity in dye inclusion. The adsorption rate difference between neutral and charged dyes implies electrostatic interactions play a key role in absorption process. The retention of charged dyes after adsorption also offers an opportunity for controllable release. This contribution is believed to bring new thoughts into MOFs design for drug delivery, large molecules separation, and dye assembly by using the host-guest interactions.
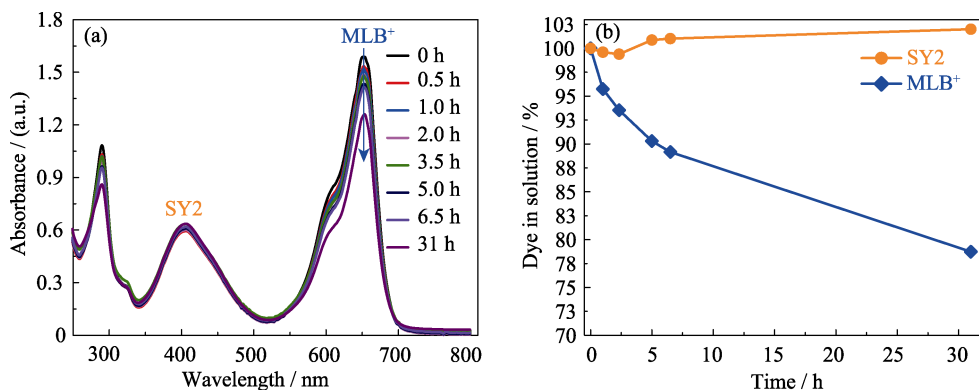
## Acknowledgements

**Fig. 4** (a) The time dependent UV-Vis spectra of the solutions of MLB$^+$ and SY2 at the ratio of 1∶1 for the competitive adsorption by Zn-MOF from 0 to 31 h ($\lambda_{max}$ = 652 nm for MlB$^+$, $\lambda_{max}$ = 406 nm for SY2); (b) The competitive adsorption rate of MIB$^+$ and SY2 by the Zn-MOF

**References:**

[1] CUI YUAN-JING, SONG RUI-JING, YU JIAN-CAN, *et al.* Dual-emitting MOF superset of dye composite for ratiometric temperature sensing. *Adv. Mater.*, 2015, **27(8):** 1420–1425.

[2] XIE WEI, HE WEN-WEN, LI SHUN-LI, *et al.* An anionic interpenetrated zeolite-like metal-organic framework composite as a tunable dual-emission luminescent switch for detecting volatile organic molecules. *Chem. Eur. J.*, 2016, **22(48):** 17298–17304.

[3] LAN YA-QIAN, JIANG HAI-LONG, LI SHUN-LI, *et al.* Mesoporous metal-organic frameworks with size-tunable cages: selective $CO_2$ uptake, encapsulation of $Ln^{3+}$ cations for luminescence, and column-chromatographic dye separation. *Adv. Mater.*, **23(43):** 5015–5020.

[4] LI PEI-ZHOU, WANG XIAO-JUN, TAN SI-YU, *et al.* Clicked isoreticular metal-organic frameworks and their high performance in the selective capture and separation of large organic molecules. *Angew. Chem., Int. Ed.*, 2015, **54(43):** 12748–12752.

[5] MA LI-QING, FALKOWSKI JOSEPH M, ABNEY CARTER, *et al.* A series of isoreticular chiral metal-organic frameworks as a tunable platform for asymmetric catalysis. *Nat. Chem.*, 2010, **2(10):** 838–846.

[6] DELLA ROCCA JOSEPH, LIU DE-MIN, LIN WEN-BIN. Nanoscale metal-organic frameworks for biomedical imaging and drug delivery. *Acc. Chem. Res.*, 2011, **44(10):** 957–968.

[7] ZHAO XIANG, MAO CHENG-YU, LUONG KAREN TU, *et al.* Framework cationization by preemptive coordination of open metal sites for anion-exchange encapsulation of nucleotides and coenzymes. *Angew. Chem., Int. Ed.*, 2016, **55(8):** 2768–2772.

[8] LIU FEI, CHUNG SO-YI, OH GAHEE, *et al.* Three-dimensional graphene oxide nanostructure for fast and efficient water-soluble dye removal. *ACS Appl. Mater. Interfaces*, 2012, **4(2):** 922–927.

[9] SIMON V, THURET A, CANDY L, *et al.* Recovery of hydroxycinnamic acids from renewable resources by adsorption on zeolites. *Chem. Eng. J.*, 2015, **280:** 748–754.

[10] ZHAO XIANG, BU XIAN-HUI, WU TAO, *et al.* Selective anion exchange with nanogated isoreticular positive metal-organic frameworks. *Nat. Commun.*, 2013, **4:** 2344–2348.

[11] HASAN ZUBAIR, JHUNG SUNG HWA. Removal of hazardous organics from water using metal-organic frameworks (MOFs): plausible mechanisms for selective adsorptions. *J. Hazard. Mater.*, 2015, **283:** 329–339.

[12] HAN YI, SHENG SHU-NAN, YANG FAN, *et al.* Size-exclusive and coordination-induced selective dye adsorption in a nanotubular metal–organic framework. *J. Mater. Chem. A*, 2015, **3(24):** 12804–12809.

[13] HAQUE ENAMUL, JUN JONG WON, JHUNG SUNG HWA. Adsorptive removal of methyl orange and methylene blue from aqueous solution with a metal-organic framework material, iron terephthalate (MOF-235). *J. Hazard. Mater.*, 2011, **185(1):** 507–511.

[14] HAN SHUANG-BING, WEI YAN-HU, CORY VALENTE, *et al.* Chromatography in a single metal-organic framework (MOF) crystal. *J. Am. Chem. Soc.*, 2010, **132(46):** 16358–16361.

[15] KANG XIAO-ZHEN, SONG ZHENG-WEI, SHI QI, *et al.* Utilization of zeolite imidazolate framework as an adsorbent for the removal of dye from aqueous solution. *Asian J. Chem.*, 2013, **25(15):** 8324–8328.

[16] LI YU, ZHOU KANG, HE MING, *et al.* Synthesis of ZIF-8 and ZIF-67 using mixed-base and their dye adsorption. *Microporous Mesoporous Mater.*, 2016, **234(1):** 287–292.

[17] QIN JUN-SHENG, ZHANG SHU-RAN, DU DONG-YING, *et al.* A microporous anionic metal-organic framework for sensing luminescence of lanthanide (III) ions and selective absorption of dyes by ionic exchange. *Chem. Eur. J.*, 2014, **20(19):** 5625–5630.

[18] SHEN XIANG, YAN BING. Anionic metal-organic framework hybrids functionalization with lanthanide ions or cationic dyes and fluorescence sensing of small molecules. *RSC Adv.*, 2016, **6(34):** 28165–28170.

[19] WU MING-YAN, JIANG FEI-LONG, WEI WEI, *et al.* A porous polyhedral metal-organic framework based on $Zn_2(COO)_3$ and $Zn_2(COO)_4$ SBUs. *Cryst. Growth Des.*, 2009, **9(6):** 2559–2561.

[20] LI HAI-CHAO, CAO XIN-YU, ZHANG CHUANG, *et al.* Enhanced adsorptive removal of anionic and cationic dyes from single or mixed dye solutions using MOF PCN-222. *RSC Adv.*, 2017, **7(27):** 16273–16281.

[21] TONG MIN-MAN, LIU DA-HUAN, YANG QING-YUAN, *et al.* Influence of framework metal ions on the dye capture behavior of MIL-100 (Fe, Cr) MOF type solids. *J. Mater. Chem. A*, 2013, **1(30):** 8534–8537.

# 具有尺寸和电荷选择性多功能分子吸附能力的电荷可转变型金属–有机框架材料

袁贝贝 [1,2,3]，周蓓蓓 [1,2,3]，章跃标 [1]，施剑林 [1,2]

(1. 上海科技大学 物质科学与技术学院, 上海 201210; 2. 中国科学院 上海硅酸盐研究所, 上海 200050; 3. 中国科学院大学, 北京 100049)

**摘 要:** 通过研究具有两种轮桨状构筑基元和四种纳米笼子结构锌基金属-有机框架(Zn-MOF)的染料吸附特性和机理, 发现其分子吸附的普适性, 以及尺寸和电荷的选择性。由于 Zn-MOF 孔道内漂浮着抗衡阴离子, 及框架上有可配位位点, 所以它能通过离子交换机理吸附阴性染料、框架上电荷转变机理吸附阳性染料、主客体相互作用吸附中性染料, 表现出优越的分子吸附多功能性。Zn-MOF 内带电荷纳米笼的尺寸选择性和电荷选择性的共同作用为设计具有更高水平兼容性和识别性的优异多孔材料铺平了道路。

**关 键 词:** 金属–有机框架; 电荷转变; 分子吸附; 选择性

**中图分类号:** TQ174　　**文献标识码:** A

Supporting information:

# Charge-switchable Metal-organic Framework for Size/Charge-selective Molecular Inclusions

YUAN Bei-Bei[1,2,3], ZHOU Bei-Bei[1,2,3], ZHANG Yue-Biao[1,3], SHI Jian-Lin[1,2,3]

(1. School of Physical Science and Technology, ShanghaiTech University, Shanghai 201210, China; 2. Shanghai Institute of Ceramics, Chinese Academy of Sciences, Shanghai 200050, China; 3. University of Chinese Academy of Sciences, Beijing 100049, China)

## General Material and Methods

5,5',5''-(((2,4,6-1,3,5-Trimethylbenzene-1,3,5-triyl)-tris(methylene))-tris(oxyl))-triisoph- thalic acid ($H_6L$) was purchased from Chemsoon; zinc nitrate tetrahydrate [$Zn(NO_3)_2 \cdot 4H_2O$] and N,N-dimethylformamide (DMF, 99.9%) were purchased from Aladdin. Anhydrous methanol (MeOH) was purchased from Sinopharm Chemical Reagent, which was used throughout all the experiments.

Solvent Yellow-2 (SY2; CAS#60-11-7) was purchased from Alfa-Aesar; Sudan-I (SD1; CAS#842-07-9), Basic Fuchsin (BF+ CAS#569-61-9), and Methyl Orange (MO-; CAS#547-58-0) were purchased from Macklin. Methylene Blue trihydrate (MLB+; CAS#7220-79-3), Crystal Violet (CV+; CAS#548-62-9), and Acid Red 88 (AR88-; CAS#1658-56-6) were purchased from Sinopharm Chemical Reagent; Acid Blue 1 (AB1-; CAS#20262-76-4), Orange G (OG2-; CAS#1936-15-8), New Coccine (NC3-; CAS#2611-82-7), and Rhodamine 6G (R6G+; CAS#989-38-8) were purchased from Aladdin; Tropaeolin OO (TOO-; CAS#554-73-4) and Acid Orange 7 (AO7-; CAS#633-96-5) were purchased from Adamas-beta.

The single-crystal X-ray diffraction data were obtained at beamline BL17B of the Shanghai Synchrotron Radiation Facility (SSRF) using X-ray with a wavelength of 0.12398 nm. The PXRD patterns were collected on a Bruker AXS D8 Phaser using Cu-K$\alpha$ radiation ($\lambda$ = 0.154050 nm) at 40 kV and 40 mA, at a scanning rate of 2.3°/min and $2\theta$ range of 3°-30°. The UV-Vis spectra were collected on an Agilent Carry5000 spectrophotometer. The optical microscope images were taken using an Optec SZ780 stereoscopic microscope equipped with a digital camera (PUDA500C).

## Syntheses of MOF

[$Zn_{14}(L)_4(H_2O)_{22}$](NO$_3$)$_4$(DMF)$_x$: In a 20 mL scintillation vial, 209 mg $H_6L$ (0.3 mmol) and 627.5 mg $Zn(NO_3)_2 \cdot 4H_2O$ (2.4 mmol) were dissolved in 16 mL DMF solution. The vial was sealed and placed in a 85℃ oven for 48 h. Colorless pyramidal crystals were obtained after cooling down to room temperature. The upper supernatant was removed and the Zn-MOF crystal at the bottom of the vial was washed with 20 mL DMF three days and three times per day. Then washed with MeOH for 5 d and three times per day.

[$Co_{14}(L)_4Cl_3(H_2O)_{22}$]Cl(DMF)$_x$:In a 20 mL scintillation vial, 209 mg $H_6L$ (0.3 mmol) and 571 mg $CoCl_2 \cdot 6H_2O$ (2.4 mmol) were dissolved in 16 mL DMF solution. The vial was sealed and placed in a 85℃ oven for 48 h. Blue-black pyramidal crystals were obtained after cooling down to room temperature. The upper supernatant was removed and the [$Co_{14}(L)_4Cl_3(H_2O)_{22}$]Cl(DMF)$_x$ crystal at the bottom of the vial was washed with 20 mL DMF three days and three times per day. Then washed with MeOH for five days and three times per day.

The crystallographic information of Zn-MOF and Co-MOF can be seen in CIF format.
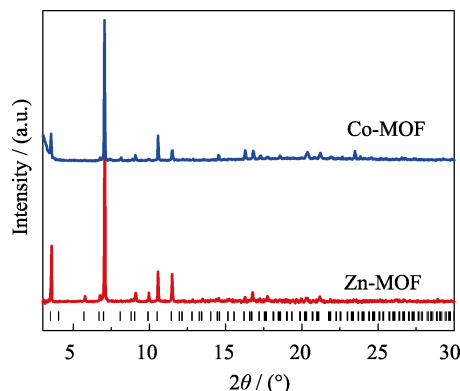


Fig. S1    PXRD patterns of Zn-MOF and Co-MOF with simulation bar. All the PXRD were carried out with a few drop of DMF on the surface
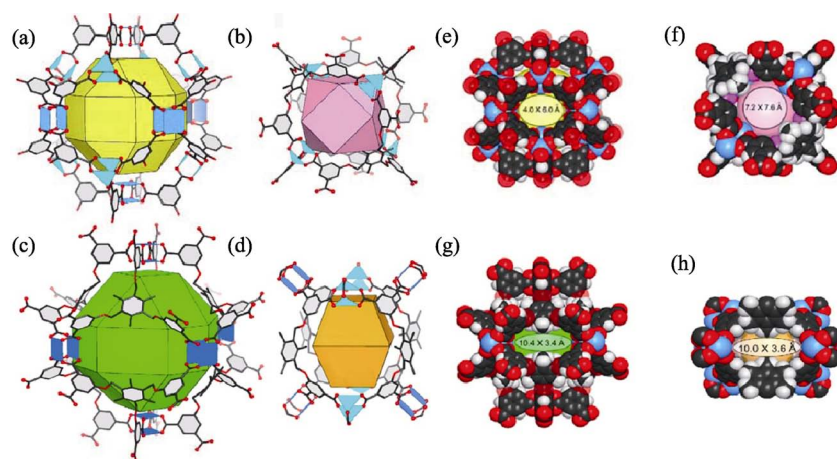
Fig. S2 (a) The rhombicuboctahedral cage enclosed alternatively by eight $Zn_2(COO)_3^+$ and six $Zn_2(COO)_4$ clusters; (b) The cuboctahedral cage enclosed by four $Zn_2(COO)_3^+$ clusters; (c) The truncated octahedral cage enclosed by six $Zn_2(COO)_4$ clusters; (d) The square-bifrustum cage enclosed alternatively by four $Zn_2(COO)_3^+$ clusters and four $Zn_2(COO)_4$ clusters. The open pores size of cages in (a), (b), (c) and (d) are (e) $0.40 \times 0.60$ nm, (f) $0.72 \times 0.76$ nm, (g) $1.04 \times 0.34$ nm and (h) $0.70 \times 0.90$ nm, respectively
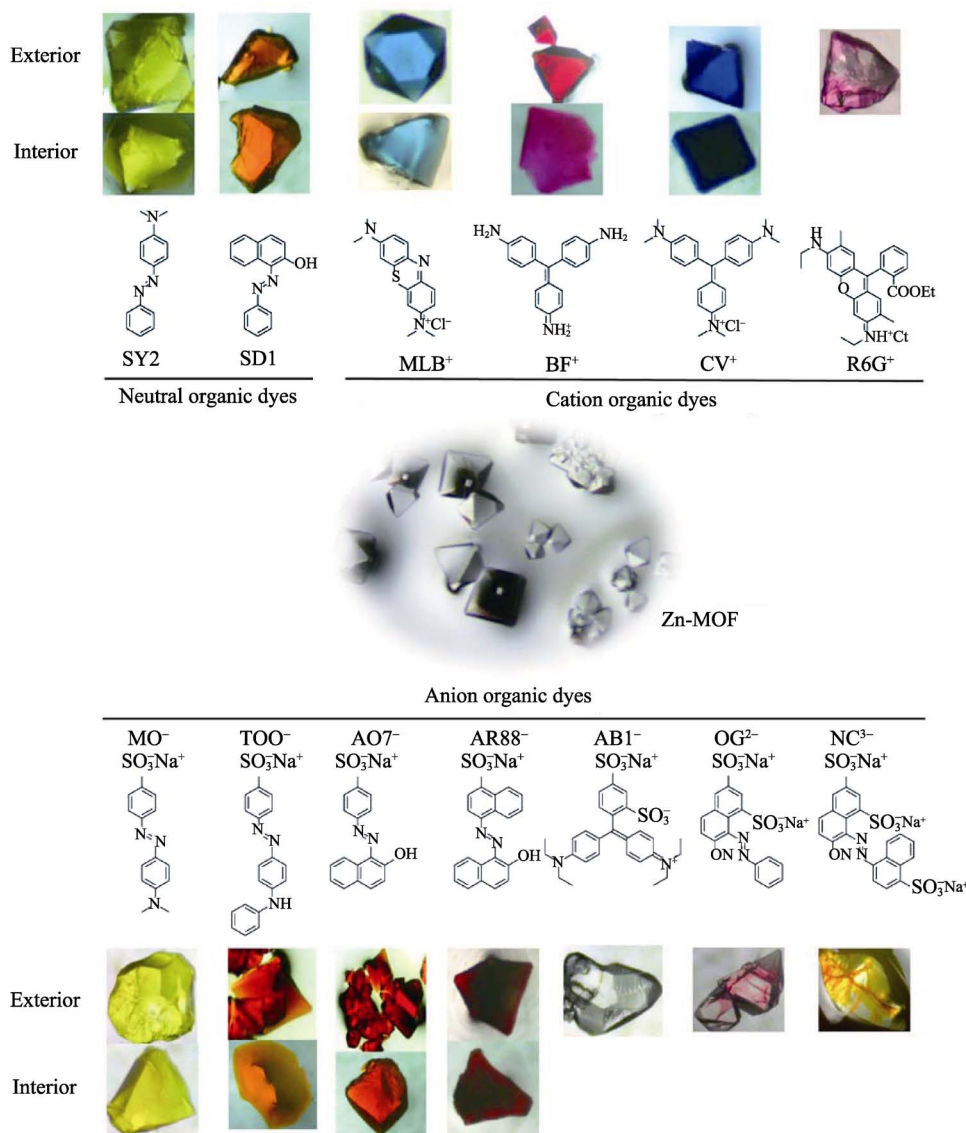


Fig. S3 The optical microscope images of the Zn-MOF crystals before (centered) and after (top and bottom) dye inclusion experiments. To confirm the uptake homogeneity of dyes, both the exterior and interior of dyes adsorbed MOF crystals were shown except those for $AB^-$, $OG^{2-}$, and $NC^{3-}$ with dyes penetrated only the outer part of the crystals
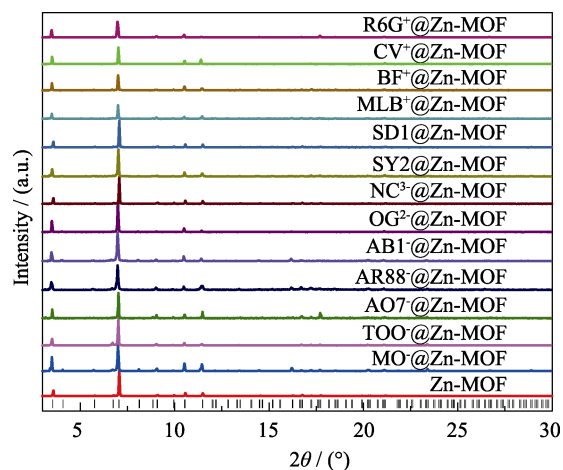
Fig. S4　PXRD patterns of Zn-MOF and dye@Zn-MOF samples compared with simulation

All the PXRD were carried out with a few drop of DMF on the surface.

It shows that the crystal structure is still maintained after adsorption of dyes
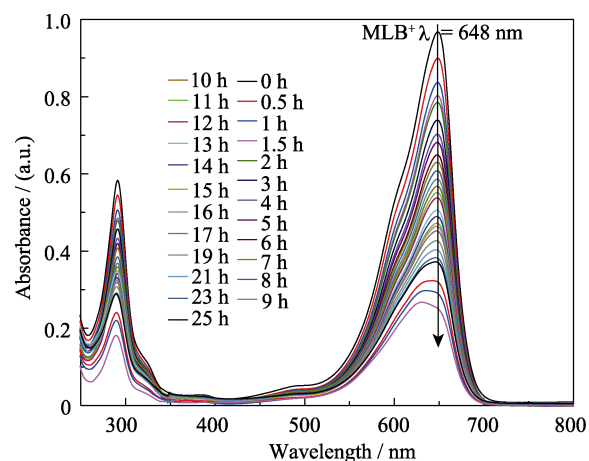


Fig. S5　The time dependent UV-Vis spectra of the solution of $MLB^+$ for adsorption by Zn-MOF from 0 to 25 h

**Table S1　Structures and dimension of guest dye molecules with different charges**

| | | | | | | | |
|---|---|---|---|---|---|---|---|
| Structure |  |  |  |  |  |  |  |
| 3D structure | | | | | | | |
| Abbr. | TOO | MO | AO7 | AR88 | AB1 | OG | NC |
| Charge | −1 | −1 | −1 | −1 | −1 | −2 | −3 |
| Inclusion | Yes | Yes | Yes | Yes | No | No | No |
| Dimension (×10⁻¹⁰, m) | $x=7.64$ $y=18.87$ $z=4.2$ | $x=15.46$ $y=8.0$ $z=5.3$ | $x=9.13$ $y=14.23$ $z=4.61$ | $x=12.9$ $y=8.63$ $z=12.9$ | $x=13.33$ $y=16.72$ $z=11.2$ | $x=11.1$ $y=12.63$ $z=4.96$ | $x=10.39$ $y=12.2$ $z=12.74$ |
| Structure | | | | | | | − |
| 3D structure | | | | | | | − |
| Abbr | SD1 | SY2 | MLB | BF | CV | R6G | − |
| Charge | 0 | 0 | +1 | +1 | +1 | +1 | − |
| Inclusion | Yes | Yes | Yes | Yes | Yes | No | − |
| Dimension (×10⁻¹⁰, m) | $x=9.32$ $y=7.58$ $z=10.89$ | $x=13.69$ $y=8.0$ $z=4.02$ | $x=15.39$ $y=8.19$ $z=3.88$ | $x=10.88$ $y=8.92$ $z=12.09$ | $x=13.72$ $y=14.65$ $z=7.47$ | $x=13.66$ $y=16.45$ $z=9.23$ | − |

**Table S2  The adsorption capacity of selected MOFs and Zn-MOF toward MLB and MO**

| MOFs | Absorption capacity/(mg·g$^{-1}$) | | Metal | Framework charge | Ref. |
|---|---|---|---|---|---|
| | Cationic dye | Anionic dye | | | |
| MOF-5 | Congo Red | NM | Zn | Neutral | [1] |
| MOF-5 | Pyronin Y, Azure A | NM | Zn | Neutral | [2] |
| ZIF-8 | 9.2 (MLB) | ~11.6 (MO) | Zn | Neutral | [3] |
| ZIF-8 | 5.4 (MLB) | 22 (AB40) | Zn | Neutral | [4] |
| IFMC-2 | MLB, CV | NA | Zn | Anionic | [5] |
| Compound 1 | MLB, RhB | NA | Zn | Anionic | [6] |
| NENU-505 | MLB, BR2 | NA | Zn | Anionic | [7] |
| Zn-MOF | 12.6 (MLB) | 19 (MO) | Zn | Cationic | This work |
| ITC-4 | NA | 77.4 (OG) | In | Cationic | [8] |
| Compound 1 | NA | 183.5 (OG) | In | Cationic | [9] |
| MOF-235 | 252.0 (MLB) | 477.0 (MO) | Fe | Cationic | [10] |
| MIL-100(Fe) | 736.2 (MLB) | 1045.2 (MO) | Fe | Cationic | [11] |
| MIL-100(Cr) | 643.3 (MLB) | 211.8 (MO) | Cr | Cationic | [11] |
| PCN-222 | 906 (MLB) | 589 (MO) | Zr | Neutral | [12] |

NM stands for not mentioned, NA stands for no absorption.

# Reference:

[1] KHANJANI SOMAYEH, MORSALI ALI. Ultrasound-promoted coating of MOF-5 on silk fiber and study of adsorptive removal and recovery of hazardous anionic dye "congo red". *Ultrason. Sonochem.* 2014, **21(4):** 1424–1429.

[2] HAN SHUANG-BING, WEI YAN-HU, CORY VALENTE, *et al.* Chromatography in a single metal-organic framework (MOF) crystal. *J. Am. Chem. Soc.*, 2010, **132(46):** 16358–16361.

[3] LI YU, ZHOU KANG, HE MING, *et al.* Synthesis of ZIF-8 and ZIF-67 using mixed-base and their dye adsorption. *Microporous Mesoporous Mater.*, 2016, **234(1):** 287–292.

[4] KANG XIAO-ZHEN, SONG ZHENG-WEI, SHI QI, *et al.* Utilization of zeolite imidazolate framework as an adsorbent for the removal of dye from aqueous solution. *Asian J. Chem.*, 2013, **25(15):** 8324–8328.

[5] QIN JUN-SHENG, ZHANG SHU-RAN, DU DONG-YING, *et al.* A microporous anionic metal-organic Framework for sensing luminescence of lanthanide (III) ions and selective absorption of dyes by ionic exchange. *Chem. Eur. J.*, 2014, **20(19):** 5625–5630.

[6] SHEN XIANG, YAN BING. Anionic metal-organic framework hybrids functionalization with lanthanide ions or cationic dyes and fluorescence sensing of small molecules. *RSC Adv.*, 2016, **6(34):** 28165–28170.

[7] ZHANG SHU-RAN, LI JING, DU DONG-YING, *et al.* A multifunctional microporous anionic metal-organic framework for column-chromatographicdye separation and selective detection andadsorption of Cr$^{3+}$. *J. Mater. Chem. A*, 2015, **3(46):** 23426–23434.

[8] ZHAO XIANG, BU XIAN-HUI, WU TAO, *et al.* Selective anion exchange with nanogated isoreticular positive metal-organic frameworks. *Nat. Commun.*, 2013(**4):** 2344–2348.

[9] SONG BAI-QIAO, WANG XIN-LONG, ZHANG YU-TENG, *et al.* Periodic tiling of triangular and square nanotubes in a cationic metal-organic framework for selective anion exchange. *Chem. Commun.*, 2015, **51(46):** 9515–9518.

[10] HAQUE ENAMUL, JUN JONGWON, JHUNG SUNGHWA. Adsorptive removal of methyl orange and methylene blue from aqueous solution with a metal−organic framework material, iron terephthalate (MOF-235). *J. Hazard. Mater.*, 2011, **185(1):** 507–511.

[11] TONG MIN-MAN, LIU DA-HUAN, YANG QING-YUAN, *et al.* Influence of framework metal ions on the dye capture behaviour of MIL-100(Fe, Cr) MOF type solids. *J. Mater. Chem. A*, 2013, **1(30):** 8534–8537.

[12] LI HAI-CHAO, CAO XIN-YU, ZHANG CHUANG, *et al.* Enhanced adsorptive removal of anionic and cationic dyes from single or mixed dye solutions using MOF PCN-222. *RSC Adv.*, 2017, **7(27):** 16273–16281.